This article has been accepted for publication in a future issue of this journal, but has not been fully edited. Content may change prior to final publication. Citation information: DOI 10.1109/TUFFC.2017.2661383, IEEE Transactions on Ultrasonics, Ferroelectrics, and Frequency Control

Coded Excitation for Pulse-Echo Systems

Julio Isla and Frederic Cegla

***Abstract*—Pulse compression has been used for decades in radar, sonar, medical and industrial ultrasound. It consists in transmitting a modulated and/or coded excitation, which is then cross-correlated with the received signal such that received echoes are time-compressed, thereby increasing their intensity and hence the system resolution and signal-to-noise ratio (SNR). A central problem in pulse-echo systems is that, while longer coded excitations yield higher SNRs, the length of the coded excitation or sequence is limited by the distance between the closest reflector and the transmitter/receiver. In this paper, a new approach to coded excitation is presented whereby receive intervals or pauses are introduced within the excitation itself; reception takes place in these intervals. As a result the code length is no longer limited by the distance to the closest reflector and a higher SNR increase can be realised. Moreover, the excitation can be coded in such a way that continuous transmission becomes possible, which reduces the overall duration of the system response to changes in the medium. The optimal distribution of the receive intervals within the excitation is discussed and an example of its application in industrial ultrasound is presented. The example consists of an electromagnetic-acoustic transducer (EMAT) driven with 4.5V, where a clear signal can be obtained in quasi-real-time (e.g. ~9Hz refresh rate) while commercially available systems require 1200V for similar performance.**

I. Introduction

Pulse-compression has been in use for decades to increase the signal-to-noise ratio (SNR) and resolution in radar [1], [2], sonar [3], [4], medical [5]–[11] and industrial ultrasound [12]–[17]. It consists of transmitting a modulated and/or coded excitation, which is then correlated with the received signal such that received echoes become shorter in duration and higher in intensity, thereby increasing the system resolution and SNR. Pulse-compression is a faster alternative to averaging because a wait time is required between consecutive excitations. During this time the energy in the medium that is being inspected dies out and therefore does not cause interference between excitations.

The two main approaches to pulse-compression are chirp signals and coded excitation (or sequences). Chirp signals are obtained by frequency-modulating the excitation; the increase in SNR and resolution depends on the chirp length and bandwidth [11]. Coded sequences operate in a slightly different way, most often by coding the polarity of concatenated bursts according to a binary sequence, i.e., a sequence composed of $1\mathrm{s}$ and $0\mathrm{s}$ or $+1\mathrm{s}$ and $-1\mathrm{s}$ [15]. In any case a good approximation to the single initial burst is obtained when correlating the received signal with the transmitted sequence, hence the term *compression*.

Julio Isla is with the Department of Mechanical Engineering, Imperial College London, UK, e-mail: j.isla13@imperial.ac.uk.

Frederic Cegla is with the Department of Mechanical Engineering, Imperial College London, UK, e-mail: f.cegla@imperial.ac.uk.

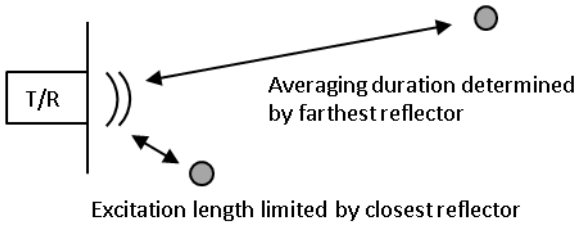

Fig. 1: Pulse-echo system with close and far reflectors.

In the applications that initially motivated this paper, namely low-power excitation of electromagnetic-acoustic transducers [12], [18], piezoelectric paints [19], photo-acoustic imaging [13], air-coupled ultrasound [14], [15], [17], [20], and guided ultrasonic waves [6], [16], the received signals lie below the noise threshold. Therefore an increase in the SNR of more than $30\,\mathrm{dB}$ is required to accurately extract the information from the signals. The goal in those scenarios is to transmit the longest sequence or chirp signal possible to achieve the highest SNR increase, but in a pulse-echo system the distance between the closest reflector and the transmit/receive source limits their length. This problem is critical when reflectors are simultaneously located very close to and very far from the transmit/receive source, see Fig. 1. In this scenario long sequences cannot be transmitted and averaging takes a longer time due to the need for long receive intervals between transmissions so that the echoes from the farthest reflector do not overlap.

Figure 2a shows a common scenario of a low-SNR pulse-echo system in industrial ultrasound affected by the problem of close and far reflectors. It consists of a metal block with a transmit-receive transducer on the front-wall of the block. The objective is to find the thickness of the block, i.e., the location of the opposite parallel back-wall. The back-wall itself acts as the closest reflector, whereas the wave reverberation between the walls behaves as reflections from far reflectors. The received signals when using averaging are shown in Fig. 2b. After each transmission there are several echoes that decay progressively and hence some wait time between transmissions is necessary to avoid interference; this makes averaging a lengthy process. Figure 2c shows the received signals when transmitting a sequence or a chirp signal. The location of the back-wall limits the length of the excitation and therefore the SNR increase. If the excitation overlaps the reflection from the back-wall, the information is lost because it is not possible to receive while transmitting.

In this paper the authors propose a solution to these problems by introducing blank gaps or intervals within a coded sequence in which reception can take place while the sequence

This article has been accepted for publication in a future issue of this journal, but has not been fully edited. Content may change prior to final publication. Citation information: DOI 10.1109/TUFFC.2017.2661383, IEEE Transactions on Ultrasonics, Ferroelectrics, and Frequency Control

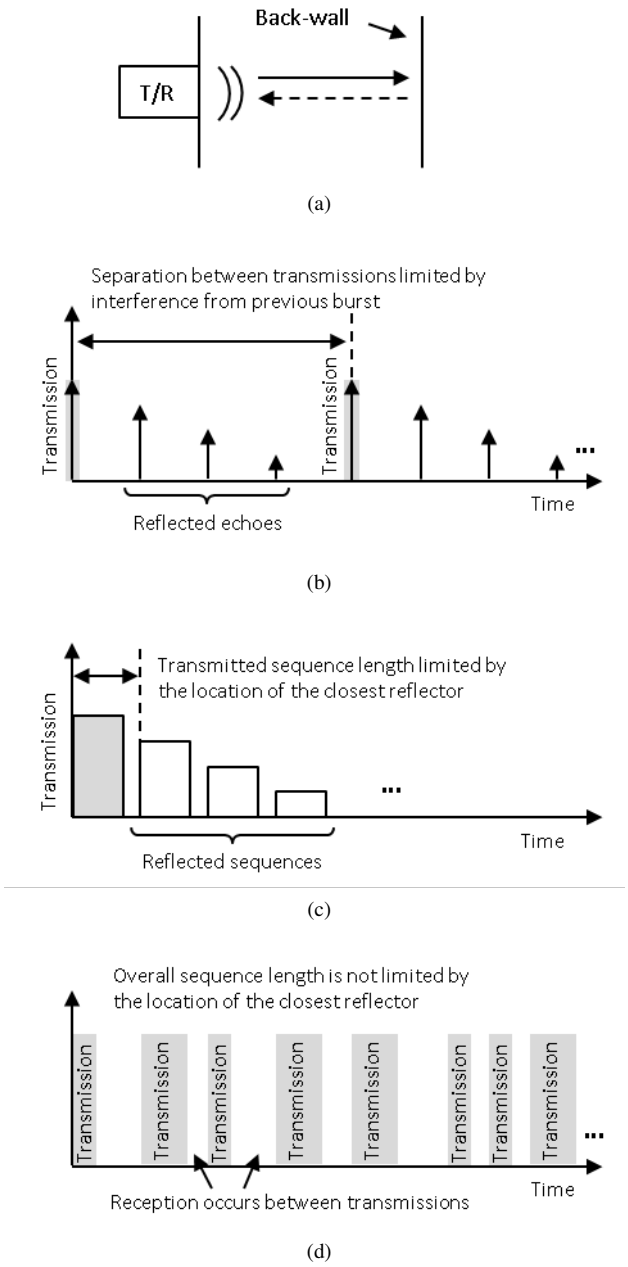

Fig. 2: Different types of excitations for pulse-echo transducers. a) Transducer operating in pulse-echo mode. b) Received signal when using averages. c) Received signals when using a sequence. d) Proposed sequence with receive intervals.

is being transmitted, see Fig. 2d. Hence, the overall sequence length and SNR increase is independent of the location of the reflectors. The aim of this idea is to increase the SNR without compromising the overall duration of the measurement so that the pulse-echo system can still respond to fast changes in the medium that is being inspected.

The organisation of this paper is as follows: first, the proposed methodology is briefly introduced. Then, the autocorrelation properties of standard sequences and the corresponding SNR increase are discussed in Sec. III. The properties and construction of coded sequences with receive intervals are introduced in Sec. IV. In Sec. V experimental results are presented. After discussing the results, conclusions are drawn.

II. Overview of proposed coded excitation

Figure 3 shows the fundamental steps of the proposed methodology. There are three main stages: 1) sequence synthesis, 2) propagation through the medium and reception, and 3) post-processing. First, two sequences are generated, sequence $\mathbf{X}$ controls the polarity of the burst ($+1$ or -1) whereas $\mathbf{G}$ controls the transmit/receive intervals (1 corresponds to transmission and 0 to reception).

In practice the transmitted sequences are not a train of delta functions but concatenated band-limited bursts, $\mathbf{B}$. These band-limited bursts are necessary due to the limited bandwidth of the electronics and transducers. The bursts are assumed to be optimal; this means that their length can be the maximum possible without overlapping the closest reflector and that they can utilise all the available bandwidth. Moreover, there is no restriction on the type of burst; they can be square pulses, chirp signals or multiple cycles with a certain apodization.

Before the sequences can be modulated by the burst $\mathbf{B}$, they have to be up-sampled by Q samples to match the burst length. By doing so $\mathbf{X}'$ and $\mathbf{G}'$ are obtained. Then $\mathbf{X}'$ is convolved with $\mathbf{B}$, which yields $\mathbf{X}''$. On the other hand $\mathbf{G}'$ is convolved with a rectangular pulse, which gives $\mathbf{G}''$. The transmitted sequence $\mathbf{Z}''$ is simply the multiplication of the elements of $\mathbf{X}''$ and $\mathbf{G}''$.

The reflected signals can be modelled as the convolution of the medium impulse response and the excited sequence $\mathbf{Z}''$; an example is shown in Fig. 3. At the receiver, the reflected signals are combined with noise from the electronics $\mathbf{Y}$. The complement $\overline{\mathbf{G}}'' = 1 - \mathbf{G}''$ is used to zero the received signal when transmission is on. This is basically the role of the transmit/receive (T/R) switch in the electronics. In practice the T/R switching occurs before the receiver noise is added to the signal; however, in Fig. 3 the order of the operation is flipped to indicate that reception does not take place during transmission and the signals are zeroed. Recall that transmission and reception cannot occur simultaneously due to the limited dynamic range of the receiver since a single transducer acts as transmitter and receiver in pulse-echo.

The modulated medium response can be partially recovered by cross-correlating the received signals with $\mathbf{X}' \cdot \mathbf{G}'$; this is the compression stage. Note that cross-correlation is equivalent to convolution with one of the terms being time-reversed. The recovered medium response will have a noise component (not shown in the figure) that corresponds to the electronics. Interference between bursts in the sequence will also affect the recovered medium response. Further noise reduction is possible by cross-correlating the result with the burst $\mathbf{B}$, which is the matched-filtering stage. However, matched filtering distorts the originally transmitted burst, as can be appreciated in the figure.

It has to be highlighted that the steps in Fig. 3 have been arranged in such a way that they correspond to fundamental steps of the methodology proposed so that it is easier to understand; however, this is not necessarily an efficient way of

This article has been accepted for publication in a future issue of this journal, but has not been fully edited. Content may change prior to final publication. Citation information: DOI 10.1109/TUFFC.2017.2661383, IEEE Transactions on Ultrasonics, Ferroelectrics, and Frequency Control

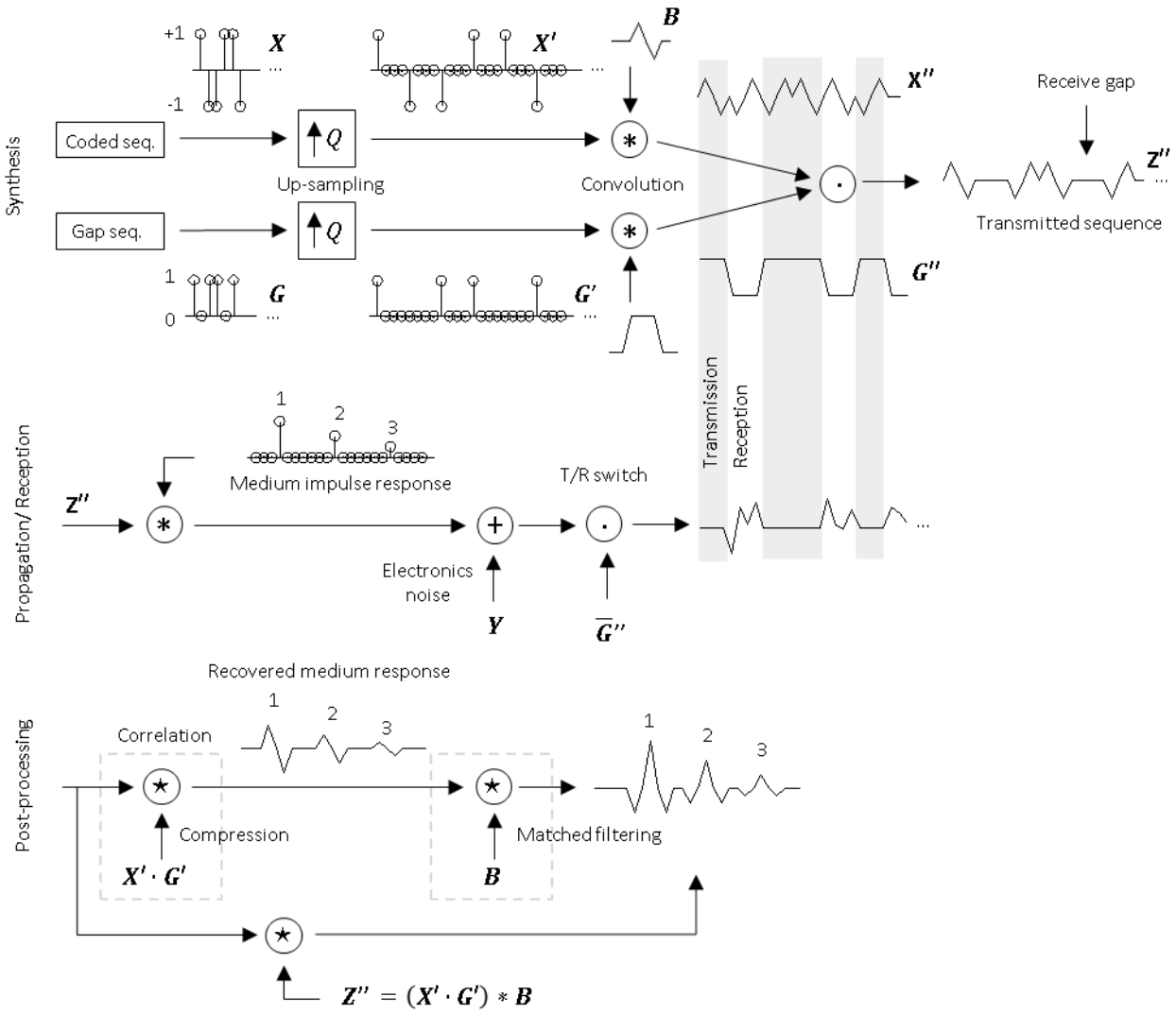

Fig. 3: Fundamental steps of the proposed coded excitation. The operators $\{\cdot\}$, $\{*\}$ and $\{\star\}$ indicate multiplication, convolution and cross-correlation respectively.

implementing it. For example, $\mathbf{Z}''$ can be obtained by simply convolving $\mathbf{B}$ with the up-sampled result of $\mathbf{X} \cdot \mathbf{G}$ and the last compression and matched-filtering operations combined, which is equivalent to cross-correlating the received signal with the transmitted signal $\mathbf{Z}'' = (\mathbf{X}' \cdot \mathbf{G}') * \mathbf{B}$, where $\{*\}$ indicates convolution.

In the next sections, we investigate the optimal synthesis of these random sequences with receive intervals and their expected SNR.

III. Background on Coded Excitation

In this section we focus our attention on coded sequences, especially binary coded sequences, whereby the polarity of the sequence burst (or symbol) is changed. These are simpler to implement than non-binary ones. There are no restrictions on the bursts other than their bandwidth not exceeding that of the system and their length not overlapping the closest reflector; note a burst can be a chirp signal. In this section we review the previous work on coded sequences and then discuss their *merit factor*; this is central to proving the optimality of the sequences with receive intervals proposed in this paper.

A. Previous work

Overall, the performance of a sequence relies on its autocorrelation properties. Ideally, its autocorrelation should be a delta function but this cannot be achieved with a single sequence. The quest for "good" sequences started around the middle of the last century [21]–[24] and still continues today [25]–[27]; see [28]–[30] for a comprehensive review of the different sequences. Among the key binary sequences known so far are those named after Barker [31], [32], and Legendre [33], as well as maximum length register sequences [34]. This list is not exhaustive and other sequences can be found in the literature [29], though some may be considered either as special cases or family members of those previously mentioned.

One of the most elegant solutions to the imperfection of the autocorrelation properties of a single sequence can be found in [21], whereby paired complementary sequences

This article has been accepted for publication in a future issue of this journal, but has not been fully edited. Content may change prior to final publication. Citation information: DOI 10.1109/TUFFC.2017.2661383, IEEE Transactions on Ultrasonics, Ferroelectrics, and Frequency Control

produce a perfect delta function when their corresponding autocorrelations are added together; this was later extended to orthogonal complementary sets of sequences in [22]. Another solution is to use sequences that achieve zero or very low autocorrelation values only in certain intervals of interest [35]–[39]. In general, there has been a tremendous interest in improving the autocorrelation properties of sequences, mainly by means of optimisation strategies, for example [26], [38]–[43], and also in efficient ways of processing and obtaining them [37], [44], [45].

The fact that good or perfect autocorrelation can be (partially) achieved is highly relevant; however, there are certain scenarios where the SNR at the input of the amplifier is low [6], [12]–[16], [18]–[20], [46], and in these cases good autocorrelation properties are not essential. Indeed, in this section it is shown that when the SNR is low (i.e., the signal magnitude is comparable to or below the noise level) the choice of the sequence is relatively unimportant and a simple random sequence that has a uniform distribution of $+1$s and -1s will suffice in most cases.

B. Merit Factor

Let $\mathbf{X}$ be a sequence of N elements, where each element x takes on values $+1$ or -1. The aperiodic autocorrelation of this sequence at shift k is

$$c_k = \sum_{j=0}^{N-k-1} x_j x_{j+k}, \qquad k = 0, \cdots, N-1. \tag{1}$$

Golay introduced the *merit factor, F,* of a sequence [47] to compare and measure its performance

$$F = \frac{N^2}{2\sum_{k=1}^{N-1} c_k^2}. \tag{2}$$

The merit factor is basically the ratio between the energy at shift zero and the combined energy of the rest of the shifts or autocorrelation sidelobes. The factor 2 is included to compensate for the tapering effect of the aperiodic autocorrelation. The merit factor can be understood as measure of how similar the autocorrelation result is to a delta function; for the sake of simplicity it should be assumed that the elements c_k, $k \in [1, N-1]$, have a zero mean. A random binary sequence with $+1$s and -1s has $F \approx 1$ on average for large N [47]; a Barker sequence of 13 elements, which is the longest known, has $F \approx 14.08$ [32], [33]; Golay sequences have $F \approx 3$, the added autocorrelations of the Golay complementary sequences have of course $F = \infty$, i.e., a delta; while Legendre sequences can achieve $F \approx 6$ [33].

Finding sequences with an optimal merit factor for a given length by extensive search is computationally demanding; the best known cases from 60 to 200 elements are limited to $F \approx 10$ [29], [30]. Longer sequences are expected to have $\max\{F\} < 6$ since no sequence with a higher merit factor has been found, though this remains a conjecture [30].

C. SNR increase

When adding (averaging) N received signals from identical excitations, the resulting SNR is

$$\mathrm{SNR}_{\mathrm{avg}} = N \cdot \mathrm{SNR}_{\mathrm{in}}, \tag{3}$$

where the input SNR, $\mathrm{SNR}_{\mathrm{in}}$, is defined as

$$\mathrm{SNR}_{\mathrm{in}} = \frac{s^2}{\sigma_{\mathrm{in}}^2}, \tag{4}$$

where s is the magnitude of the received signal, assuming that the excitation is an impulse and that there is only one point-like reflector, and σ_{in}^2 is the variance of the received noise, which has zero mean. In most ultrasound systems, the received noise is mainly due to electrical noise of the receive amplifier – for simplicity this noise can be assumed to be additive white Gaussian noise. Clearly the actual received signal can take on other values after noise is added, but here s refers to the ideal received signal prior to additive noise.

In order to simplify the analysis and to focus the attention on the sequences themselves two assumptions have been made: a) the excitation is an impulse and b) there is only one point-like reflector. This means that the receive sequence only takes on $+s$ and $-s$ values. We then discuss the effect of modulation and multiple reflectors in Sec. IV-F.

When using coded excitation, the cross-correlation of the received signal and the transmitted sequence introduces noise as a result of the interference between the coded bursts in the sequence. This interference is of (pseudo) random nature and behaves similarly to the electrical noise of the receiver. Therefore, it is referred to simply as noise and measured in the same way since its effect is not different from that of electrical noise.

Let the transmitted sequence be of length N with unity magnitude and let the received sequence take on values $+s$ and $-s$. Then, the energy at shift $k = 0$ after cross-correlation is $(N \cdot s)^2$, while the sample variance of the noise introduced by the cross-correlation is σ_s^2, which can be defined as

$$\sigma_s^2 = \frac{2s^2}{N-1} \sum_{k=1}^{N-1} c_k^2 \approx \frac{N \cdot s^2}{F}, \tag{5}$$

when N is large. The factor 2 in equation (5) has been added to compensate for the tapering effect the aperiodic cross-correlation has on c_k.

Now let $\mathbf{Y}$ be a sequence of independent and identically (normally) distributed (i.i.d.) elements y_j with zero mean and variance σ^2; say this sequence represents the noise added at the receiver. The sample variance of the result of cross-correlating $\mathbf{Y}$ with the transmitted sequence can be approximated, if N is large, to

$$\sigma_{\mathrm{Y}}^2 \approx \mathrm{E}\left[\frac{2}{N-1} \sum_{k=1}^{N-1} d_k^2\right] \tag{6}$$

where $\mathrm{E}[\cdot]$ denotes the expected value and d_k are the coefficients of the cross-correlation for each shift k. Since each d_k is i.i.d with zero mean

This article has been accepted for publication in a future issue of this journal, but has not been fully edited. Content may change prior to final publication. Citation information: DOI 10.1109/TUFFC.2017.2661383, IEEE Transactions on Ultrasonics, Ferroelectrics, and Frequency Control

$$\sigma_{\mathrm{Y}}^2 \approx \frac{2}{N-1}\sum_{k=1}^{N-1}\mathrm{E}\left[d_k^2\right], \tag{7}$$

$$d_k = \sum_{j=0}^{N-k-1} y_j x_{j+k}, \qquad k \in [1, N-1]. \tag{8}$$

Due to each y_j and x_{j+k} being also i.i.d. with zero mean,

$$\begin{aligned}\mathrm{E}\left[d_k^2\right] &= \textstyle\sum_{j=0}^{N-k-1}\mathrm{E}\left[y_j^2\right]\mathrm{E}\left[x_{j+k}^2\right] \\ &= \sigma^2(N-k), \qquad k \in [1, N-1]\end{aligned} \tag{9}$$

Hence,

$$\sigma_Y^2 \approx N\sigma^2. \tag{10}$$

Finally, given that the noise introduced by the sequence is independent of the noise introduced by $\mathbf{Y}$, the SNR of the aperiodic cross-correlation can be approximated, when N is large, as

$$\mathrm{SNR_s} = \frac{(N\cdot s)^2}{\sigma_s^2+\sigma_Y^2} \approx \frac{N}{\frac{1}{F}+\frac{1}{\mathrm{SNR_{in}}}}. \tag{11}$$

There are two special cases of interest in equation (11)

$$\mathrm{SNR_s} \approx \begin{cases} N\cdot\mathrm{SNR_{in}} & if\ F \gg \mathrm{SNR_{in}} \\ N\cdot F & if\ F \ll \mathrm{SNR_{in}} \end{cases}. \tag{12}$$

If $F \gg \mathrm{SNR_{in}}$, the SNR increase due to coded excitation is that of averaging – see equation (3). Moreover, *there is no benefit in using sequences with $F > 1$ (i.e., other than random sequences, which achieve $F \approx 1$ when N is large) to increase the SNR when* $\mathrm{SNR_{in}} \ll 1$. Note that even the complementary Golay sequences, which can perfectly cancel the sequence noise [21], [22], yield no advantage in this case.

Interestingly, many scenarios exist where either $\mathrm{SNR_{in}} \sim 1$ or $\mathrm{SNR_{in}} \ll 1$ and hence a significant number of averages or long sequences are required (commonly $N > 1000$) to produce a satisfactory SNR, which often needs to be in the order of $30-50\,\mathrm{dB}$. These scenarios are usually found in systems that rely on inefficient/poor transducers or constraints on the excitation power [6], [12]–[16], [18]–[20], [46].

Conversely, if $F \ll \mathrm{SNR_{in}}$, the $\mathrm{SNR_s}$ is independent of $\mathrm{SNR_{in}}$, and if $\mathrm{SNR_{in}}$ is high, it may happen that $\mathrm{SNR_{in}} > \mathrm{SNR_s}$ for a given N due to the noise introduced by the sequence during the cross-correlation operation. In these cases special attention should be paid to increasing the merit factor F and hence to the use of complementary Golay sequences and zero autocorrelation zone sequences [35]–[39].

IV. Properties and Synthesis of Sequences with Receive Intervals

In a pulse-echo system the length of the excitation, be that a coded sequence or a chirp signal, is limited by the distance between the closest reflector and the transmit/receive source, see Fig. 1. In order to transmit longer sequences, intervals – where reception can take place – can be introduced in the sequences. In this section the rationale behind this approach is explained and the optimal distribution of the receive intervals within a given sequence is discussed.

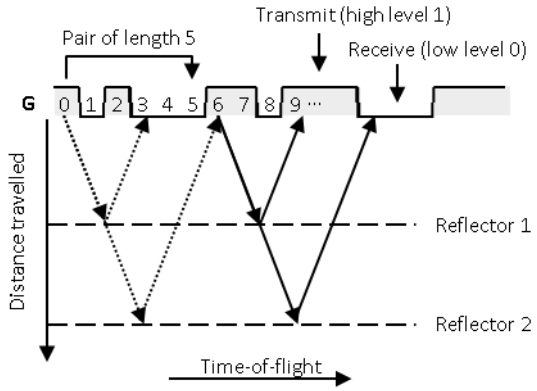

Fig. 4: Random distribution of receive intervals in a sequence. A burst is sent in each transmit interval (sequence $\mathbf{G}$ high level) and the reflected echo can be received only if its arrival time matches the occurrence of a receive interval (sequence $\mathbf{G}$ low level).

A. Synthesis of sequences with receive intervals

It is desirable to create a ternary random sequence $\mathbf{Z}$ that takes on values $+1$, -1, and 0, where the values $+1$ and -1 codify the excitation and the zeroes permit reception to take place, hence the name gap or receive interval. Such a ternary sequence can be synthesised as follows. Let $\mathbf{X}$ be a binary sequence of length L that takes on values $+1$ and -1 and let $\mathbf{G}$ be another binary sequence also of length L that takes on values $+1$ and 0. Sequence $\mathbf{Z}$ can be obtained as

$$\mathbf{Z} = \mathbf{X}\cdot\mathbf{G} = (x_0g_0, x_1g_1, \ldots, x_{L-1}g_{L-1}), \tag{13}$$

where each x_j and g_j are i.i.d.. The process described by equation (13) was shown in Fig. 3 but including the burst modulation. The sequence $\mathbf{G}$ controls the location of the receive intervals ($g_j = 0$) and transmit intervals ($g_j = 1$), whereas $\mathbf{X}$ controls the polarity (±1) of the bursts during the transmit interval. For simplicity, and without loss of generality, each transmit/receive intervals is considered to be of the same length. The expected SNR when using $\mathbf{Z}$ is quantified in Sec. IV-C, where each term of equation (13) is instrumental in the mathematical formulation.

Now we introduce the concept of transmit-receive pairs within the sequence $\mathbf{G}$. The transmit-receive pairs are responsible for the amount of energy received from reflectors, which is discussed in Sec. IV-B. Let $\overline{g}_j$ be the complement of g_j defined as

$$\overline{g}_j = 1 - g_j, \tag{14}$$

then $\{g_j, g_{j+m}\}$ *is said to be a transmit-receive pair of length* m if $g_j\overline{g}_{j+m} = 1$. As an example, a pair of length $m = 5$ is shown in Fig. 4.

The pair length is defined as a range of time differences between any two transmit and receive states. Therefore, a

This article has been accepted for publication in a future issue of this journal, but has not been fully edited. Content may change prior to final publication. Citation information: DOI 10.1109/TUFFC.2017.2661383, IEEE Transactions on Ultrasonics, Ferroelectrics, and Frequency Control

given pair length corresponds to the total travel time range of a wave to and back from a potential reflector. The larger the pair length, the longer the travel time, and hence the deeper the potential reflector. The amount of energy received from a given reflector is proportional to the total number of transmit and receive pairs of a pair length that corresponds to the depth of the reflector. For this reason, a uniform probability distribution of pair lengths is desired in order to have a uniform sensitivity with respect to the reflector depth. In the next section it is discussed how to ensure this condition, whereas the expected amount of energy received from a given reflector is investigated in Sec. IV-C.

Figure 4 shows an example of a sequence $\mathbf{G}$ together with the time-of-flight and distance travelled by waves generated in transmit intervals of $\mathbf{G}$. For example, the wave generated in g_0 reflects back from reflectors 1 and 2 and the first reflection arrives at g_3, so this reflector location is said to require a pair of length $m = 3$. Equally, the second reflection arrives at g_6 and hence this reflector is said to require a pair $m = 6$.

In a pulse-echo system, where transmission and reception cannot occur simultaneously due to the limited dynamic range of the receiver, a transmit-receive pair may not exist for a given transmit interval and reflector location. For example, in Fig. 4 $\{g_0, g_6\}$ is not a valid pair because $g_0\overline{g}_6 = 0$ and hence the reflection cannot be received.

B. Random distribution of receive and transmit intervals for even sampling of the medium

In a pulse echo system it is important to ensure equal sensitivity to every reflector regardless of its location in the interrogated space. When using the sequences with receive intervals and ignoring beam spread and directivity effects, this is equivalent to obtaining the same number of reflections, i.e. the same amount of energy, from any point-like reflector irrespective of its location. More formally, this is to obtain the same number of reflections r for any transmit-receive pair of length m up to a length M.

This condition can approximately be satisfied by any random binary sequence $\mathbf{G}$ when L is large and $L \gg M$. To prove this, let the expected number of reflections that correspond to a reflector, whose distance from the transducer corresponds to a transmit-receive pair of length m, be

$$r_m = \mathrm{E}\left[\sum_{j=0}^{L-m-1} g_j \overline{g}_{j+m}\right] \qquad m \in [1, M]\,. \tag{15}$$

Note that r_m is basically the expected total number of valid transmit-receive pairs, i.e., those that yield $g_j\overline{g}_{j+m} = 1$, for each shift m.

Let p_1 be the probability of having a transmit interval defined as

$$p_1 = \mathrm{E}\left[g_j\right] = 1 - \mathrm{E}\left[\overline{g}_j\right]. \tag{16}$$

As every g_j in equation (15) is i.i.d.,

$$r_m = p_1\left(1 - p_1\right)(L - m) \qquad m \in [1, M]\,. \tag{17}$$

Then if $L \gg M$,

$$r = r_m|_{L\gg M} \approx p_1\left(1 - p_1\right)L. \tag{18}$$

In practice the location of the furthest reflector is limited to an equivalent transmit-receive pair of length M. By using sequences of length $L \gg M$, the number of reflections from any possible reflector location within such a finite distance can be homogenised, as shown by equation (18). This greatly simplifies the formulae for the quantification of the sequence SNR in the next section.

C. SNR and optimal ratio of transmit and receive intervals

Having discussed that a random distribution of transmit-receive intervals guarantees that the same number of reflections r be received irrespective of the reflector location within a finite distance from the source, the next step is to investigate the optimal number or proportion of transmit-receive intervals in a sequence, i.e., find the optimal p_1. The optimal number of transmit intervals p_1L is that which yields the maximum SNR for a given sequence $\mathbf{G}$ of length L. To obtain the SNR of a sequence with receive intervals, the total received energy, the noise from the sequence and the added noise at the receiver need to be found as follows.

Let $\mathbf{Y}$ be the noise added at the receiver. To estimate the sample variance after the cross-correlation of $\mathbf{Y}$ with the transmitted sequence $\mathbf{Z}$, σ^2_{YG}, the steps from equations (6) to (10) can be repeated. When M is large, σ^2_{YG} can be approximated as

$$\sigma^2_{YG} \approx \frac{1}{M}\sum_{k=1}^{M} e_k^2 \approx \mathrm{E}\left[e_k^2\right] \qquad M \ll L. \tag{19}$$

where e_k are the coefficients of the cross-correlation for each shift k. Note that the factor 2 has been dropped with respect to equation (6) because $M \ll L$ shifts are used to obtain σ^2_{YG} and therefore the tapering effect of the cross-correlation can be neglected.

$$\mathrm{E}\left[e_k^2\right] = \sum_{j=0}^{L-k-1} \mathrm{E}\left[z_j^2\overline{g}_{j+k}y_{j+k}^2\right], \qquad k \in [1, M]\,, \tag{20}$$

where $z_j = x_jg_j$ are the elements of $\mathbf{Z}$ and $\overline{g}_jy_j$ are the elements of the received sequence; note that $\overline{g}_j^2 = \overline{g}_j$. Finally

$$\sigma^2_{\mathrm{YG}} \approx r\sigma^2 \qquad M \ll L. \tag{21}$$

Now the sample variance of the noise introduced by the sequence itself is investigated following the same steps. Say M is large, then

$$\sigma^2_{SG} \approx \frac{1}{M}\sum_{k=1}^{M} f_k^2 \approx \mathrm{E}\left[f_k^2\right] \qquad M \ll L, \tag{22}$$

where f_k are the coefficients of the cross-correlation for each shift k and

This article has been accepted for publication in a future issue of this journal, but has not been fully edited. Content may change prior to final publication. Citation information: DOI 10.1109/TUFFC.2017.2661383, IEEE Transactions on Ultrasonics, Ferroelectrics, and Frequency Control

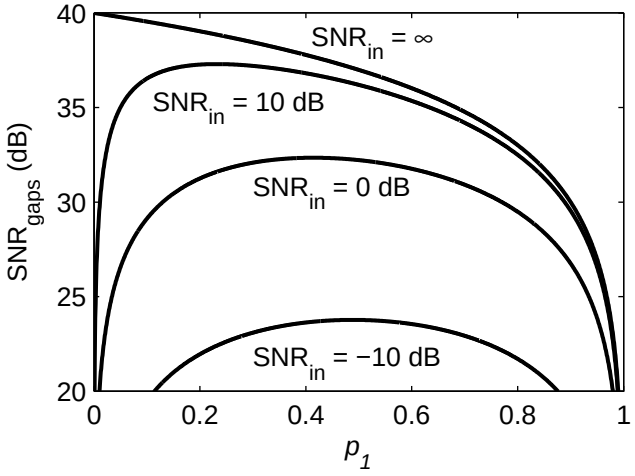

Fig. 5: SNR of the sequence with receive intervals, $\mathrm{SNR}_{\mathrm{gaps}}$, vs. the probability of having a transmit interval, p_1, for different input SNRs, $\mathrm{SNR}_{\mathrm{in}}$. The total length of the sequence is set to $L = 10^4$.

$$\mathrm{E}\left[f_k^2\right] = s^2 \sum_{j=m}^{L-k-1} \mathrm{E}\left[z_j^2 \overline{g}_{j+k} z_{j-m+k}^2\right], \qquad m \in [1, M], \tag{23}$$

where $z_{j-m}s = g_{j-m}x_{j-m}s$ are the elements of the reflected sequence (i.e., the transmitted sequence z_j scaled by s and shifted by m) while the actual received sequence is $\overline{g}_j z_{j-m} s$. Note that

$$\sigma_{SG}^2 \approx p_1 r s^2 \qquad M \ll L. \tag{24}$$

According to equation (18), r reflections are received and since each reflection has magnitude s, the total received energy at shift $k = m$ is approximately $(r \cdot s)^2$ when $L \gg M$. Hence, when M is large and $L \gg M$,

$$\mathrm{SNR}_{\mathrm{gaps}} \approx \frac{(r \cdot s)^2}{\sigma_{SG}^2 + \sigma_{YG}^2} \approx \frac{r}{p_1 + \frac{1}{\mathrm{SNR}_{\mathrm{in}}}}. \tag{25}$$

Figure 5 shows $\mathrm{SNR}_{\mathrm{gaps}}$ vs. p_1 for different $\mathrm{SNR}_{\mathrm{in}}$; L has been set to 10^4 to provide a numerical example. There are two extreme cases of interest

$$\mathrm{SNR}_{\mathrm{gaps}} \approx \begin{cases} r \cdot \mathrm{SNR}_{\mathrm{in}} & if\, \mathrm{SNR}_{\mathrm{in}} \ll \frac{1}{p_1} \\ (1 - p_1)\, L & if\, \mathrm{SNR}_{\mathrm{in}} \gg \frac{1}{p_1} \end{cases} \tag{26}$$

Given that $\max\{r\} = 0.25L$, which occurs for $p_1 = 0.5$, then $\max\{\mathrm{SNR}_{\mathrm{gaps}}\}|_{\mathrm{SNR}_{\mathrm{in}} \ll 2} = 0.25L \cdot \mathrm{SNR}_{\mathrm{in}}$. Conversely, if $\mathrm{SNR}_{\mathrm{in}} \gg \frac{1}{p_1}$, $\mathrm{SNR}_{\mathrm{gaps}}$ is independent of $\mathrm{SNR}_{\mathrm{in}}$, and if $\mathrm{SNR}_{\mathrm{in}}$ is high, it may happen that $\mathrm{SNR}_{\mathrm{in}} > \mathrm{SNR}_{\mathrm{gaps}}$, in which case the use of the sequences is detrimental.

Moreover, $\mathrm{SNR}_{\mathrm{gaps}}$ is a concave function of p_1 for any $\mathrm{SNR}_{\mathrm{in}} < \infty$. Then, there exists a value of p_1 that maximises $\mathrm{SNR}_{\mathrm{gaps}}$ for each $\mathrm{SNR}_{\mathrm{in}}$

$$p_{1,\max} = \arg\max_{p_1} \{\mathrm{SNR}_{\mathrm{gaps}}\} \leq 0.5 \tag{27}$$

and hence the maximum $\mathrm{SNR}_{\mathrm{gaps}}$ is

$$\mathrm{SNR}_{\mathrm{gaps,max}} \approx \frac{(1 - p_{1,\max})\, L}{1 + \frac{1}{p_{1,\max}\mathrm{SNR}_{\mathrm{in}}}}. \tag{28}$$

An important fact is that $p_1 = 0.5$ performs nearly optimal once $\mathrm{SNR}_{\mathrm{in}} < 0\,\mathrm{dB}$.

The figure of merit of the sequence F was not included in equation (25) because this equation is intended to be used with random sequences that do not have any predefined structure and for which $F \approx 1$ when L is large. This is because we conjecture that it should be difficult to obtain a sequence that produces $F > 1$ when random receive intervals are used due to the structure of the transmitted sequence being affected by these intervals.

Finally, it is worth mentioning that sequences whose elements take on values $+1$, -1 and 0 have been reported in the literature and are known as ternary sequences [48]–[50]. However, the insertion of the zeroes aims to improve the sequence autocorrelation properties and is not initially intended for reception to take place. Furthermore, these sequences do not necessarily satisfy $p_1 = 0.5$, which is required when $\mathrm{SNR}_{\mathrm{in}} \ll 2$.

D. Comparison between sequences with receive intervals and averaging

Once we assume that the sequence burst is optimal (i.e., their length can be the maximum possible without overlapping the closest reflector and they can utilise all the available bandwidth) and that the sequence burst can also be a chirp signal, averaging using the same sequence burst is the only relevant comparison point against the sequences with receive intervals. In this section we investigate which of these techniques yields the highest SNR increase in a given amount of time subject to initial conditions. To do so, we introduce the following ratio

$$\alpha = \frac{\mathrm{SNR}_{\mathrm{gaps,max}}}{\mathrm{SNR}_{\mathrm{avg}}} \approx \frac{1 - p_{1,\max}}{t\left(\mathrm{SNR}_{\mathrm{in}} + \frac{1}{p_{1,\max}}\right)}, \tag{29}$$

$$t = \frac{N}{L}, \tag{30}$$

where L is the total number number of transmit and receive intervals for both the sequences and averaging, which corresponds to the total duration of the measurement. For the case of averaging, N is the number of averages that take place during the L intervals; the number of receive intervals $(L - N)$ is dictated by the need of a wait time to allow the waves in the medium to die out and hence avoid interference between averages. For example, if $t = \frac{1}{4}$, then the wait time between averages necessary to avoid interference is 4 intervals or less (1 transmit and 3 receive intervals). Note that the number of transmit intervals in a sequence of length L is $p_1 L$, or $p_{1,\max} L$ in the case of equation (29). As before, transmit and receive intervals are considered of equal length without loss of generality.

Figure 6 shows the values of t and $\mathrm{SNR}_{\mathrm{in}}$ for which $\alpha \approx 1$. For any combination of t and $\mathrm{SNR}_{\mathrm{in}}$ values below the curve, $\alpha > 1$, and hence the sequences with receive intervals produce

This article has been accepted for publication in a future issue of this journal, but has not been fully edited. Content may change prior to final publication. Citation information: DOI 10.1109/TUFFC.2017.2661383, IEEE Transactions on Ultrasonics, Ferroelectrics, and Frequency Control

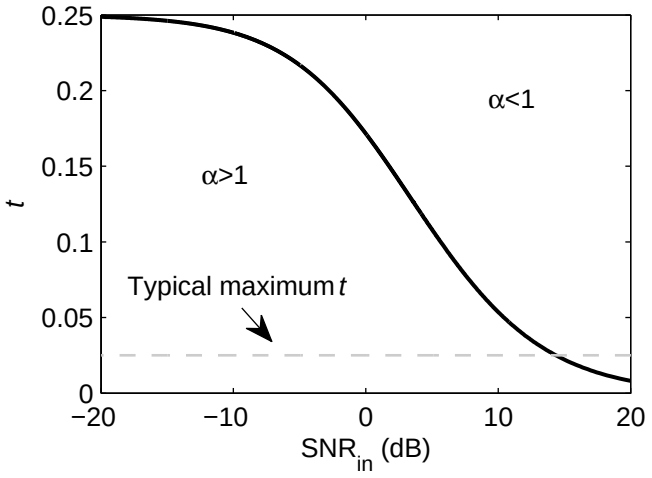

Fig. 6: Ratio of transmit and total number of intervals when averaging, $t = \frac{N}{L}$, and input SNR, $\mathrm{SNR}_{\mathrm{in}}$, for which the SNR obtained after using the sequences with receive intervals is approximately the same to that of averaging, i.e., $\alpha \approx 1$. For any combination of t and $\mathrm{SNR}_{\mathrm{in}}$ values below the curve, $\alpha > 1$, and hence the sequences with receive intervals produce a greater SNR than averaging. The dashed grey line corresponds a typical maximum t showing that for inputs with $\mathrm{SNR}_{\mathrm{in}} < 10\,\mathrm{dB}$ the sequences with receive intervals outperform averaging.

a greater SNR; otherwise, averaging produces a higher SNR. A desired t for a given $\mathrm{SNR}_{\mathrm{in}}$ may not be achieved when averaging due to many receive intervals being required to avoid interference between transmissions, e.g., when wave reverberations inside the specimen are significant.

Consider the extreme case in equation (29) where $\mathrm{SNR}_{\mathrm{in}} \ll 2$ and for which $p_1 = 0.5$ is known to be optimal, then

$$\alpha|_{\mathrm{SNR}_{\mathrm{in}} \ll 2, p_1 = 0.5} \approx \frac{1}{4t}. \tag{31}$$

This means that when $\mathrm{SNR}_{\mathrm{in}} \ll 2$ and $t < \frac{1}{4}$, i.e., when the wait time between averages necessary to avoid interference is greater than 4 intervals (1 transmit and 3 receive intervals), the sequence with receive intervals produces a greater SNR. Finding scenarios where there is no interference using 3 or less receive intervals when averaging is rare in practice. A common scenario in pulse-echo ultrasound systems is to use more than 40 receive intervals when averaging – the receiver is on for 40 times the transmit length to avoid interference. In such a case the SNR achieved by the sequence can be at least $20\,\mathrm{dB}$ greater provided $\mathrm{SNR}_{\mathrm{in}} \ll 2$ and $p_1 = 0.5$.

E. Periodic sequences with receive intervals: continuous transmission

Let the sequence $\widehat{\mathbf{Z}}$ be infinite with period L and elements

$$\widehat{z}_{j+qL} = z_j \qquad j \in [0, L-1]\,, \tag{32}$$

where q is an integer and the elements z_j are defined in equation (13). In the same way $\widehat{g}_j$ can be defined from g_j.

Say $\widehat{\mathbf{Z}}$ is transmitted and the received signal is cross-correlated with $\widehat{\mathbf{Z}}$ shifted by n. The expected value of the periodic cross-correlation of a finite number of samples L is then

$$\begin{aligned} &\mathrm{E}\left[\widehat{f}_{k,n}\right] = s\sum_{j=0}^{L-1}\mathrm{E}\left[\widehat{z}_{j-n}\overline{\widehat{g}}_{j-n+k}\widehat{z}_{j-m+k}\right] \\ &= \begin{cases} r\cdot s & k = m-n+qL \\ 0 & otherwise \end{cases}, \qquad m,k \in [1, L-1] \end{aligned}. \tag{33}$$

Since $\widehat{\mathbf{Z}}$ and $\widehat{\mathbf{G}}$ have period L, for every n there exists a value of k in the interval $[1, L-1]$ for which $\mathrm{E}\left[\widehat{f}_{k,n}\right] = r\cdot s$. This means that the sequence $\widehat{\mathbf{Z}}$ can be transmitted continuously and at any instant n reflections within a time-of-flight of $m < L-1$ can be recovered after cross-correlating L received elements. Note the same $\mathrm{SNR}_{\mathrm{gaps}}$ is obtained when replacing $\mathbf{Z}$ by $\widehat{\mathbf{Z}}$.

By transmitting a sequence with finite period L, a significant amount of memory and computing power is saved but the time-of-flight of the furthest reflection has to be less than $L-1$ to prevent these reflections from being seen as coherent interference. This is equivalent to waiting for the energy in a specimen to die out between transmissions when using averaging. The importance of being able to transmit/receive continuously is that it significantly reduces any delays in the system when processing the sequences, which then reduces the time the system takes to respond to changes in the medium.

F. Burst modulation and multiple reflectors

Let s_i be the magnitude of the received echo from reflector i, then equation (25) can be rewritten for a reflector i' as

$$\mathrm{SNR}'_{\mathrm{gaps}} \approx \frac{L\,(1-p_1)}{\sum_{i=1}^{R} s_i^2 + \frac{1}{p_1 \mathrm{SNR}_{\mathrm{in}}}}, \tag{34}$$

where R is the total number of reflectors, the reflectors are assumed to be well resolved, and $\mathrm{SNR}_{\mathrm{in}}$ is defined with respect to $s_{i'}$. The existence of multiple reflectors increases the sequence noise; however, this increase is not significant if there are just a few dominant reflectors, as happens to be the case in most practical scenarios.

To include the effect of the burst modulation, let us assume that: the sequences are up-sampled to match the burst length, as shown in Fig. 3; that the normalised modulated burst $\mathbf{B}$ has variance σ_B^2 and mean zero; and that the received sequences are correlated with the up-sampled but unmodulated sequences $\mathbf{X}' \cdot \mathbf{G}'$ in the compression stage as shown in Fig. 3. This process can be understood as a shifted combination of the transmitted sequence weighted by the burst samples. Since only the peak of the burst is of interest in the numerator, this process has no effect on it. Note that only the transmitted sequences are modulated, which has no effect on the right hand term of the denominator either. Hence the result of the modulation on transmission is simply the variance σ_B^2 multiplying the left hand term of the denominator

$$\mathrm{SNR}''_{\mathrm{gaps}} \approx \frac{L\,(1-p_1)}{\sigma_B^2 \sum_{i=1}^{R} s_i^2 + \frac{1}{p_1 \mathrm{SNR}_{\mathrm{in}}}}. \tag{35}$$

This article has been accepted for publication in a future issue of this journal, but has not been fully edited. Content may change prior to final publication. Citation information: DOI 10.1109/TUFFC.2017.2661383, IEEE Transactions on Ultrasonics, Ferroelectrics, and Frequency Control

Typically $\sigma_B^2 \sim 0.2$ for normalised bursts, so modulation reduces the sequence noise at the expense of longer excitations.

It should be highlighted that discontinuities may occur between adjacent intervals. The magnitude of the discontinuities is given by a) the difference in the number of reflections of two contiguous transmit-receive pair lengths – for very long sequences this difference is negligible and can also be compensated on the post-processing stage because the number of reflections from every transmit-receive pair length is known a priori – and b) the phase change of the electronics noise between non-adjacent receive intervals due to the noise being band-limited. Overall, the effect of these discontinuities is negligible and can be further attenuated by filtering.

An additional SNR increase is possible by using matched filtering, see Fig. 3. The effect of matched filtering on the SNR can be found elsewhere, e.g. [51]. Basically if the signal is assumed to have a white noise component, mainly due to the electronics noise, the increase in the SNR corresponds to the energy of the burst. However, this result cannot be immediately extrapolated to the noise introduced by the sequences because it mostly shares the same frequency band of the burst. We found empirically that an acceptable approximation of the resulting sequence noise (left hand term of the denominator) is as follows

$$\mathrm{SNR}'''_{\mathrm{gaps}} \approx \frac{L\,(1-p_1)\,Q\sigma_B^2}{2Q\sigma_B^2\sigma_{BB}^2\sum_{i=1}^{R} s_i^2 + \frac{1}{p_1\mathrm{SNR}_{\mathrm{in}}}}, \qquad (36)$$

where Q is the number of samples of the burst and σ_{BB}^2 is the variance of the normalised auto-correlation of the burst. It is interesting to note that when the left hand term of the denominator is negligible, which corresponds to a regime where the sequences perform optimally, the SNR increase due to matched filtering is $Q\sigma_B^2$, i.e., the energy of the burst.

V. Application example: fast low-power EMAT

In this section a sequence with receive intervals was applied to an industrial ultrasound example, which consists of an electromagnetic-acoustic transducer (EMAT) driven with only $4.5\,\mathrm{Vpp}$ (peak-to-peak) and less than $0.5\,\mathrm{W}$. The main advantage of using EMATs is that, unlike standard piezoelectric transducers, they do not require direct contact with the specimen. However, EMATs are notorious for requiring very high excitation voltages, commonly in excess of a few hundred volts and powers greater than $1\,\mathrm{kW}$ [52]–[56]. In certain scenarios high powers are not permissible, e.g. in explosive environments, such as refineries, or where compact/miniaturised electronics is wanted. Moreover, high-power electronics requires bigger components and more space to dissipate the heat. The use of sequences with receive intervals presented in this paper can be used to reduce the excitation power while keeping the overall duration of the measurement short in these scenarios.

A. Experimental Setup

The experiment setup is shown in Fig. 7a-b. An EMAT (Part No. 274A0272, Innerspec, USA) was placed on top of a mild steel block, which had a thickness of $20\,\mathrm{mm}$. This is a pancake coil EMAT that generates radially polarised shear waves within a circular aperture, which has an outer diameter of roughly $20\,\mathrm{mm}$.

The main objective of this setup is to obtain a signal that can be used to estimate the thickness of the steel block. In this particular case it is convenient to use the coded sequences with receive intervals because a) the back-wall can be close and therefore long chirp signals or standard sequences cannot be used and b) the steel block offers low attenuation to the wave, which reverberates inside the specimen for a long time, making averaging lengthy due to the wait time needed between transmissions.

A custom-made transmit-receive electronic circuit was developed for the experiment. This circuit was solely powered by the USB port of a standard personal computer (PC), which can deliver a maximum of $5\,\mathrm{V}$ and $5\,\mathrm{W}$. The electronics consists of a balanced transmitter with a maximum output voltage of $4.5\,\mathrm{Vpp}$ and maximum output current of $150\,\mathrm{mA}$, hence the maximum peak power is less than $0.34\,\mathrm{W}$. The receiver provided a gain of roughly $60\,\mathrm{dB}$ and both transmitter and receiver have a bandwidth greater than $5\,\mathrm{MHz}$.

A device (Handyscope-HS5, TiePie , Netherlands) that consists of a signal generator and an analog-to-digital converter (ADC) was employed to drive the custom-made transmitter (driver) and to digitise the output of the custom-made receive amplifier. The Handyscope-HS5 communicates with a PC via the USB port. Both the signal generator and the ADC of the Handyscope-HS5 were sampled at $100\,\mathrm{MHz}$.

In a second setup, the EMAT was connected to the transmit-receive system PowerBox H (Innerspec, USA) – provided by the manufacturer of the EMAT – without changing the EMAT position on the steel block. This setup is not shown for the sake of brevity. The PowerBox H was set to drive the EMAT at $1200\,\mathrm{Vpp}$, which according to the manufacturer can produce a peak power of $8000\,\mathrm{W}$. A 3-cycle pulsed burst at a central frequency of $2.5\,\mathrm{MHz}$ was transmitted. The number of averages in the system was set to zero and the repetition rate to 30 bursts per second to avoid any interference from subsequent excitations. The receive amplifier gain was set to $60\,\mathrm{dB}$.

B. Results

The signals obtained using the PowerBox H (Innerspec, USA) were matched-filtered with a 3-cycle Hanning window centred at $2.5\,\mathrm{MHz}$ to produce a fairer comparison with the cross-correlation output of the sequences; the output of the filter is shown in Fig. 8a. Multiple echoes that correspond to the back- and front-walls of the steel block can be observed to decay progressively. Smaller echoes produced by mode conversion (from shear to longitudinal waves and vice versa) can also be observed between the main echoes. These mode-coverted echoes act as coherent noise, which is dominant over the electrical random noise of the electronics. Therefore, there is not much gain in increasing any further the transmitted power, the length of the sequence or the number of averages in order to increase the SNR because the coherent noise will increase proportionally.

This article has been accepted for publication in a future issue of this journal, but has not been fully edited. Content may change prior to final publication. Citation information: DOI 10.1109/TUFFC.2017.2661383, IEEE Transactions on Ultrasonics, Ferroelectrics, and Frequency Control

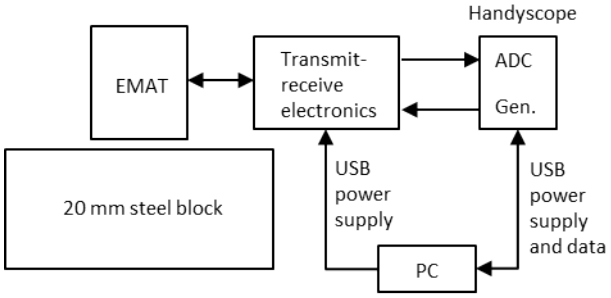

(a)

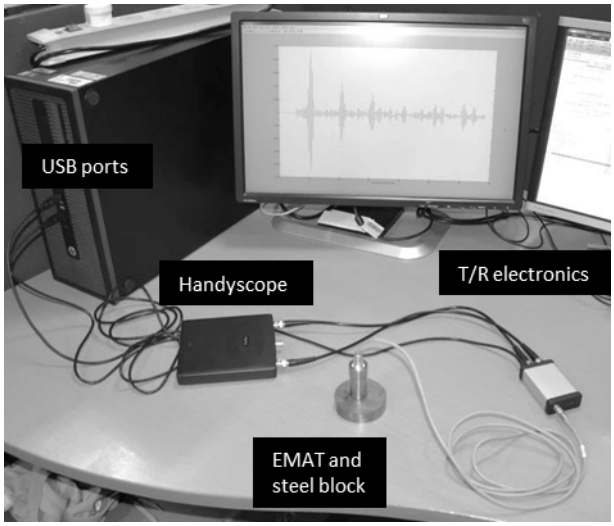

(b)

Fig. 7: Experimental setup using low-power custom-made electronics and sequences with receive intervals to drive a commercial EMAT employing $4.5\,\mathrm{Vpp}$ only. a) Block diagram. b) Photograph of real setup.

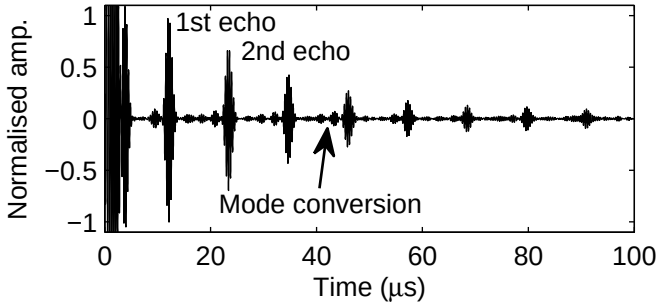

(a) Innerspec system ($1200\,\mathrm{Vpp}$).

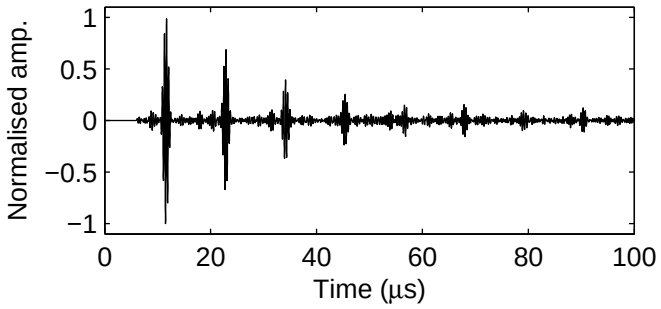

(b) Low-power custom-made system ($4.5\,\mathrm{Vpp}$).

Fig. 8: Echoes from $20\,\mathrm{mm}$-thick steel block. a) Signal from the Innerspec system using $1200\,\mathrm{Vpp}$ excitation. b) Signal from custom-made electronics using a sequence with receive intervals. Signals are normalised to the maximum value of the first echo.

To drive the custom-made electronics shown in Fig. 7b) a sequence of length $2^{14} = 16384$ was generated with equal number of receive and transmit intervals randomly distributed as described in Fig. 3. The sequence burst consisted of a 3-cycle Hanning window centred at $2.5\,\mathrm{MHz}$ similarly to the excitation used for the PowerBox H. The length of the sequence intervals was set to 6 times the burst duration totalling $7.2\,\mu\mathrm{s}$; this produces a blind zone of roughly $10\,\mathrm{mm}$ within a steel specimen when using a shear-wave transducer. This was necessary to permit the energy in the transducer to die out, so that the receive electronics does not saturate. Overall, the total duration of the sequence was $118\,\mathrm{ms}$. The authors argue that a system that processes the data at this rate can be considered quasi-real-time for inspections that use hand-held transducers.

The received signals were zeroed at the transmission intervals to eliminate any noise introduced during this stage and then correlated with the transmitted sequence, see Fig. 3; the results are shown in Fig. 8b. The first echoes can be clearly identified from the noise threshold. In general, the noise level of Fig. 8b appears to be, by visual inspection, just slightly greater than that of Fig. 8a. This noise could either be noise introduced by the sequence or random electrical noise – the latter mainly due to the receive amplifier. Nonetheless, it is clear that a similar performance can be achieved even with a drastic reduction in the excitation power.

To investigate the performance of the sequence in more detail, an EMAT that produces shear waves linearly polarised [18] was used instead. This EMAT achieves a higher mode purity and a more collimate radiation pattern, so that a thicker sample can be used where the echoes are well separated and mode conversion can be considered negligible. The new specimen is an aluminium block with dimension $80\times80\times150\,\mathrm{mm}^3$, and the transducer was placed in the middle of one of the $80 \times 150\,\mathrm{mm}^2$ faces.

All the parameters remained the same except for the sampling frequency, which was reduced to $20\,\mathrm{MHz}$, so that the acquisition system can handle longer sequences. First, $2^{17} = 131072$ signals were averaged; the result is shown in Fig. 9a, where the inset shows the transmitted burst. The objective was to find a region in the signal where the dominant source of noise corresponds to the receive electronics. Ring down from the coil, noise from the T/R switches and mode conversion can be observed before the first echo, but after the first echo the noise from the receive electronics dominates. Hence, a good approximation can be obtained by computing

This article has been accepted for publication in a future issue of this journal, but has not been fully edited. Content may change prior to final publication. Citation information: DOI 10.1109/TUFFC.2017.2661383, IEEE Transactions on Ultrasonics, Ferroelectrics, and Frequency Control

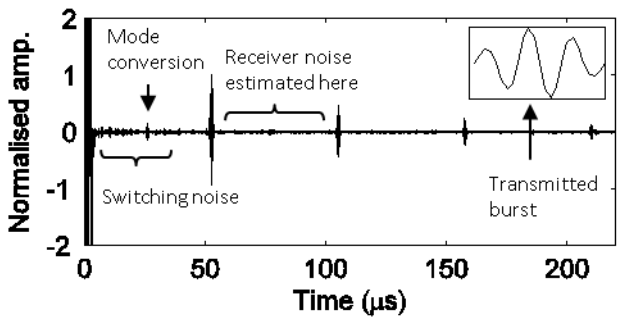

(a) 2^{17} averages.

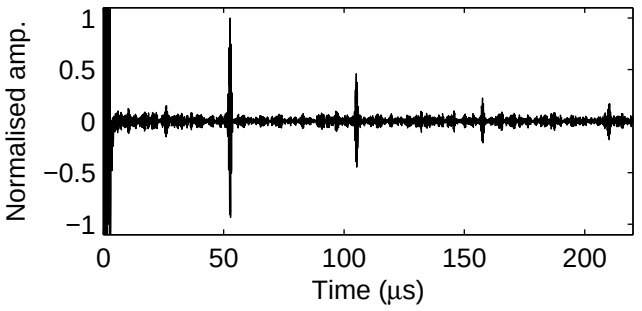

(b) 2^{14} averages.

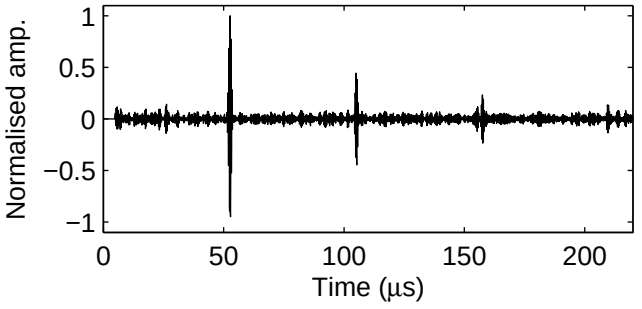

(c) Sequence of length 2^{16}.

Fig. 9: Signals using linearly polarised shear wave EMAT [18]. a) 2^{17} averages; the inset shows the transmitted burst. b) 2^{14} averages. c) Sequence of length 2^{16}.

the variance of the noise between the first two echoes, as indicated by the horizontal brace.

Figure 9b shows the signals after $N = 2^{14}$ averages and the result being cross-correlated with the excitation burst. In this input SNR regime a signal with the same output SNR can be obtained by using a sequence that has a length $L = 2^{16} = 65536$ and intervals 6 times longer than the transmitted burst, as shown in Fig. 9c.

The SNR after averaging $N = \{2^{10}, 2^{12}, 2^{14}\}$ signals and convolving the result with the excited burst is shown in Fig. 10 with circle markers. The SNR produced by sequences of length $L = \{2^{12}, 2^{13}, \ldots, 2^{17}\}$ with intervals 6 times longer than the transmitted burst is shown with asterisk markers.

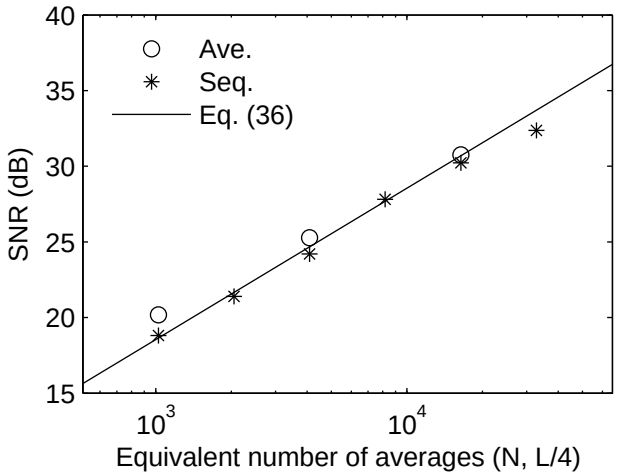

Fig. 10: Experimentally observed SNR vs. number of averages N or equivalent sequence length $L/4$. The input SNR is $\mathrm{SNR_{in}} = -19.5\,\mathrm{dB}$.

To evaluate equation (36), so that experimental and theoretical results can be compared, the input SNR, $\mathrm{SNR_{in}}$, was estimated from the SNR of the resulting signal after $N = 2^{14}$ averages by dividing it by the number of averages and the variance of the burst $\sigma_B^2 = 0.26$ and the number of samples of the burst $Q = 25$; this yielded $\mathrm{SNR_{in}} = -19.5\,\mathrm{dB}$. Also, the variance of the normalised auto-correlation of the burst was $\sigma_{BB}^2 = 0.16$ and the sum of the peak value of the first four echoes normalised to the first one was $\sum_{i=1}^{4} s_i^2 \approx 1.3$. With all this information at hand, the output of equation (36) was plotted in Fig. 10 for different L values as shown by the continuous line. Overall there is good agreement between the SNRs obtained using averaging, the sequences (with intervals 6 times longer than the burst duration) and equation (36).

It should be noted that under this low input SNR regime ($\mathrm{SNR_{in}} = -19.5\,\mathrm{dB}$), the right hand term of denominator of equation (36) is predominant over the left hand term, therefore the noise introduced by the sequence itself is insignificant. Moreover, note that in this case the increase in the sequence noise due to the multiple reflectors is less than 30%.

C. Discussion of results

The main conclusion from the experiments is that a significant power reduction in the excitation can be obtained by using coded sequences with receive intervals while still being able to obtain a quasi-real-time response. Note that had averaging been used with the custom-made electronics, the wait time between transmissions would have needed to be around $1000\,\mu s$ and the number of averages needed $2^{12} = 4096$, which corresponds to a total duration of around $4\,\mathrm{s}$ (40 times longer than the sequences).

The power delivered by the PowerBox H was expected to be in the order of $8000\,\mathrm{W}$. A similar signal was obtained by the custom-made electronics driven with the proposed sequences using a mere $0.34\,\mathrm{W}$, which corresponds to a difference of more than $40\,\mathrm{dB}$. The exact power reduction achieved

by the custom-made electronics when using the sequences (compared to the PowerBox H) should be interpreted with care because the noise performance of the receive electronics of both systems has a direct impact on the SNR of the received signal; note the noise performance of the PowerBox H and the custom-made electronics were not compared.

The importance of fast and quiet switching electronics and also of active damping in procuring a short transmission interval should be highlighted. A drawback of the custom-made electronics employed was that the transmission interval was excessively large (6 times the duration of the excitation burst). This was necessary to attenuate any remaining energy in the EMAT coil after the excitation and to prevent the receive amplifier from entering into saturation during reception. In this is paper both transmit and receive intervals were set to the same length to simplify the analysis. However, when large transmission intervals are necessary to wait for any ring down or switching noise to die out, it should be considered to only increase the length of those transmit intervals that are followed by a receive interval.

It is also worth mentioning that when the received signals lie close to or below the noise threshold, as in [6], [12]–[16], [18]–[20], [46], analog-to-digital converters (ADCs) can be replaced by comparators with negligible ($2\,\mathrm{dB}$) loss of information [46], [57]–[59]. This may result in a faster, more compact and efficient electronics.

VI. Conclusions

Pulse-compression has been used for decades to increase the SNR without significantly increasing the overall duration of the measurement but current pulse-compression techniques cannot be used in pulse-echo when a significant SNR increase is needed and there are close reflectors. This paper presents a solution to that problem, which consists in inserting gaps in a coded sequence where reception can take place.

When the input SNR is low ($< 10\,\mathrm{dB}$) or there are far reflectors present, the sequences with receive intervals are much faster than averaging or can produce an extra SNR increase for the same overall measurement duration. In general, the sequences can outperform averaging by more than $20\,\mathrm{dB}$ in many cases.

We also show that under low input SNR a simple random codification of the sequence using equal number of receive and transmit intervals of equal length randomly distributed performs optimally. Moreover, a sequence of any given length can be continuously transmitted without pauses, which increases the refresh rate of the system.

An application of these sequences in industrial ultrasound was presented. It was shown that an EMAT can be driven with $4.5\,\mathrm{Vpp}$ obtaining a clear signal in quasi-real-time; commercially available systems require $1200\,\mathrm{Vpp}$ for similar performance.

Future work should be related to the development of fast-switching electronics and the use of the proposed sequences with receive intervals in parallel channels as in medical/industrial ultrasound arrays, where their pseudo-orthogonality can be exploited.

Data accessibility

Readers who are interested in accessing data associated with this paper are referred to www.imperial.ac.uk/non-destructive-evaluation where either the data or details of how to obtain the data can be found.

Acknowledgements

J. Isla would like to thank Prof. P. Cawley for comments on the manuscritp. F. Cegla would like to acknowledge funding from EPSRC, grant reference EP/K033565/1.

References

[1] A. S. Mudukutore, V. Chandrasekar, and R. J. Keeler, "Pulse compression for weather radars," *Geoscience and Remote Sensing, IEEE Transactions on*, vol. 36, no. 1, pp. 125–142, 1998.

[2] M. Parlak, M. Matsuo, and J. F. Buckwalter, "Analog signal processing for pulse compression radar in 90-nm cmos," *Microwave Theory and Techniques, IEEE Transactions on*, vol. 60, no. 12, pp. 3810–3822, 2012.

[3] K. Nakahira, T. Kodama, T. Furuhashi, and H. Maeda, "Design of digital polarity correlators in a multiple-user sonar ranging system," *Instrumentation and Measurement, IEEE Transactions on*, vol. 54, no. 1, pp. 305–310, 2005.

[4] Y.-T. Tseng, J.-J. Ding, and C.-S. Liu, "Analysis of attenuation measurements in ocean sediments using normal incidence chirp sonar," *Oceanic Engineering, IEEE Journal of*, vol. 37, no. 3, pp. 533–543, 2012.

[5] D. Maresca, K. Jansen, G. Renaud, G. Van Soest, X. Li, Q. Zhou, N. de Jong, K. K. Shung, and A. Van der Steen, "Intravascular ultrasound chirp imaging," *Applied Physics Letters*, vol. 100, no. 4, p. 043703, 2012.

[6] X. Song, D. Ta, and W. Wang, "A base-sequence-modulated golay code improves the excitation and measurement of ultrasonic guided waves in long bones," *Ultrasonics, Ferroelectrics and Frequency Control, IEEE Transactions on*, vol. 59, no. 11, pp. 2580–2583, 2012.

[7] C.-C. Shen and C.-H. Lin, "Chirp-encoded excitation for dual-frequency ultrasound tissue harmonic imaging," *Ultrasonics, Ferroelectrics and Frequency Control, IEEE Transactions on*, vol. 59, no. 11, 2012.

[8] C. Yoon, W. Lee, J. Chang, T.-K. Song, and Y. Yoo, "An efficient pulse compression method of chirp-coded excitation in medical ultrasound imaging," *Ultrasonics, Ferroelectrics, and Frequency Control, IEEE Transactions on*, vol. 60, no. 10, pp. 2225–2229, 2013.

[9] T. Harrison, A. Sampaleanu, and R. Zemp, "S-sequence spatially-encoded synthetic aperture ultrasound imaging [correspondence]," *Ultrasonics, Ferroelectrics and Frequency Control, IEEE Transactions on*, vol. 61, no. 5, pp. 886–890, 2014.

[10] S. Mensah, J. Rouyer, A. Ritou, and P. Lasaygues, "Low-contrast lesion detection enhancement using pulse compression technique," *The Journal of the Acoustical Society of America*, vol. 135, no. 4, pp. 2156–2156, 2014.

[11] T. Misaridis and J. A. Jensen, "Use of modulated excitation signals in medical ultrasound. part iii: high frame rate imaging," *Ultrasonics, Ferroelectrics, and Frequency Control, IEEE Transactions on*, vol. 52, no. 2, pp. 208–219, 2005.

[12] K. Ho, T. Gan, D. Billson, and D. Hutchins, "Application of pulse compression signal processing techniques to electromagnetic acoustic transducers for noncontact thickness measurements and imaging," *Review of scientific instruments*, vol. 76, no. 5, p. 054902, 2005.

[13] M. Mienkina, C.-S. Friedrich, N. Gerhardt, W. Wilkening, M. Hofmann, and G. Schmitz, "Experimental evaluation of photoacoustic coded excitation using unipolar golay codes," *Ultrasonics, Ferroelectrics and Frequency Control, IEEE Transactions on*, vol. 57, no. 7, pp. 1583–1593, 2010.

[14] T. Gan, D. Hutchins, D. Billson, and D. Schindel, "The use of broadband acoustic transducers and pulse-compression techniques for air-coupled ultrasonic imaging," *Ultrasonics*, vol. 39, no. 3, pp. 181–194, 2001.

[15] M. Ricci, L. Senni, and P. Burrascano, "Exploiting pseudorandom sequences to enhance noise immunity for air-coupled ultrasonic nondestructive testing," *Instrumentation and Measurement, IEEE Transactions on*, vol. 61, no. 11, pp. 2905–2915, 2012.

[16] J. E. Michaels, S. J. Lee, A. J. Croxford, and P. D. Wilcox, "Chirp excitation of ultrasonic guided waves," *Ultrasonics*, vol. 53, no. 1, pp. 265–270, 2013.

[17] D. Hutchins, P. Burrascano, L. Davis, S. Laureti, and M. Ricci, "Coded waveforms for optimised air-coupled ultrasonic nondestructive evaluation," *Ultrasonics*, 2014.

[18] J. Isla and F. Cegla, "Optimisation of the bias magnetic field of shear wave emats," *Ultrasonics, Ferroelectrics, and Frequency Control, IEEE Transactions on*, Doi 10.1109/TUFFC.2016.2558467.

[19] B. Yoo, A. Purekar, Y. Zhang, and D. Pines, "Piezoelectric-paint-based two-dimensional phased sensor arrays for structural health monitoring of thin panels," *Smart Materials and Structures*, vol. 19, no. 7, p. 075017, 2010.

[20] R. J. Przybyla, S. E. Shelton, A. Guedes, I. Izyumin, M. H. Kline, D. Horsley, B. E. Boser, *et al.*, "In-air rangefinding with an aln piezoelectric micromachined ultrasound transducer," *Sensors Journal, IEEE*, vol. 11, no. 11, pp. 2690–2697, 2011.

[21] M. J. Golay, "Complementary series," *Information Theory, IRE Transactions on*, vol. 7, no. 2, pp. 82–87, 1961.

[22] C.-C. Tseng and C. Liu, "Complementary sets of sequences," *Information Theory, IEEE Transactions on*, vol. 18, no. 5, pp. 644–652, 1972.

[23] R. Sivaswamy, "Multiphase complementary codes," *Information Theory, IEEE Transactions on*, vol. 24, no. 5, pp. 546–552, 1978.

[24] J. M. Jensen, H. E. Jensen, and T. Hoholdt, "The merit factor of binary sequences related to difference sets," *Information Theory, IEEE Transactions on*, vol. 37, no. 3, pp. 617–626, 1991.

[25] L. Xu and Q. Liang, "Zero correlation zone sequence pair sets for mimo radar," *Aerospace and Electronic Systems, IEEE Transactions on*, vol. 48, no. 3, pp. 2100–2113, 2012.

[26] M. Soltanalian and P. Stoica, "Computational design of sequences with good correlation properties," *Signal Processing, IEEE Transactions on*, vol. 60, no. 5, pp. 2180–2193, 2012.

[27] Z. Liu, Y. L. Guan, and W. H. Mow, "A tighter correlation lower bound for quasi-complementary sequence sets," *Information Theory, IEEE Transactions on*, vol. 60, no. 1, pp. 388–396, 2014.

[28] P. Borwein, K.-K. S. Choi, and J. Jedwab, "Binary sequences with merit factor greater than 6.34," *Information Theory, IEEE Transactions on*, vol. 50, no. 12, pp. 3234–3249, 2004.

[29] J. Jedwab, "A survey of the merit factor problem for binary sequences," in *Sequences and Their Applications-SETA 2004*, pp. 30–55, Springer, 2005.

[30] J. Jedwab, "What can be used instead of a barker sequence?," *Contemporary Mathematics*, vol. 461, pp. 153–178, 2008.

[31] R. H. Barker, "Group synchronization of binary digital systems in communication theory," *Academic Press, New York*, 1953.

[32] K. H. Leung and B. Schmidt, "The field descent method," *Designs, Codes and Cryptography*, vol. 36, no. 2, pp. 171–188, 2005.

[33] T. Hoholdt and H. E. Jensen, "Determination of the merit factor of legendre sequences," *Information Theory, IEEE Transactions on*, vol. 34, no. 1, pp. 161–164, 1988.

[34] S. W. Golomb and G. Gong, *Signal design for good correlation: for wireless communication, cryptography, and radar*. Cambridge University Press, 2005.

[35] H. Torii, M. Nakamura, and N. Suehiro, "A new class of zero-correlation zone sequences," *Information Theory, IEEE Transactions on*, vol. 50, no. 3, pp. 559–565, 2004.

[36] P. Fan, W. Yuan, and Y. Tu, "Z-complementary binary sequences," *Signal Processing Letters, IEEE*, vol. 14, no. 8, pp. 509–512, 2007.

[37] M. C. Pérez, J. Ureña, Á. Hernández, A. Jiménez, and C. De Marziani, "Efficient generation and correlation of sequence pairs with three zero-correlation zones," *Signal Processing, IEEE Transactions on*, vol. 57, no. 9, pp. 3450–3465, 2009.

[38] J. Song, P. Babu, and D. Palomar, "Sequence design to minimize the weighted integrated and peak sidelobe levels," 2015.

[39] J. Song, P. Babu, and D. P. Palomar, "Optimization methods for designing sequences with low autocorrelation sidelobes," *Signal Processing, IEEE Transactions on*, vol. 63, no. 15, pp. 3998–4009, 2015.

[40] P. Stoica, H. He, and J. Li, "New algorithms for designing unimodular sequences with good correlation properties," *Signal Processing, IEEE Transactions on*, vol. 57, no. 4, pp. 1415–1425, 2009.

[41] H. He, P. Stoica, and J. Li, "On aperiodic-correlation bounds," *Signal Processing Letters, IEEE*, vol. 17, no. 3, pp. 253–256, 2010.

[42] W. Nam and S.-H. Kong, "Least-squares-based iterative multipath super-resolution technique," *Signal Processing, IEEE Transactions on*, vol. 61, no. 3, pp. 519–529, 2013.

[43] M. Soltanalian, M. M. Naghsh, and P. Stoica, "On meeting the peak correlation bounds," *Signal Processing, IEEE Transactions on*, vol. 62, no. 5, pp. 1210–1220, 2014.

[44] C. De Marziani, J. Ureña, Á. Hernández, M. Mazo, F. J. Álvarez, J. J. García, and P. Donato, "Modular architecture for efficient generation and correlation of complementary set of sequences," *Signal Processing, IEEE Transactions on*, vol. 55, no. 5, pp. 2323–2337, 2007.

[45] E. Garcia, J. Ureña, and J. J. García, "Generation and correlation architectures of multilevel complementary sets of sequences," *Signal Processing, IEEE Transactions on*, vol. 61, no. 24, pp. 6333–6343, 2013.

[46] J. Isla and F. Cegla, "The use of binary quantisation for the acquisition of low snr ultrasonic signals: a study of the input dynamic range," *Ultrasonics, Ferroelectrics, and Frequency Control, IEEE Transactions on*, DOI 10.1109/TUFFC.2016.2571843.

[47] M. J. Golay, "Sieves for low autocorrelation binary sequences," *Information Theory, IEEE Transactions on*, vol. 23, no. 1, pp. 43–51, 1977.

[48] T. Hoholdt and J. Justesen, "Ternary sequences with perfect periodic autocorrelation (corresp.)," *Information Theory, IEEE Transactions on*, vol. 29, no. 4, pp. 597–600, 1983.

[49] A. Gavish and A. Lempel, "On ternary complementary sequences," *Information Theory, IEEE Transactions on*, vol. 40, no. 2, pp. 522–526, 1994.

[50] R. Craigen and C. Koukouvinos, "A theory of ternary complementary pairs," *Journal of Combinatorial Theory, Series A*, vol. 96, no. 2, pp. 358–375, 2001.

[51] B. A. Carlson, "Introduction to communication systems," 2001.

[52] P. Wilcox, M. Lowe, and P. Cawley, "Omnidirectional guided wave inspection of large metallic plate structures using an emat array," *Ultrasonics, Ferroelectrics, and Frequency Control, IEEE Transactions on*, vol. 52, no. 4, pp. 653–665, 2005.

[53] R. Ribichini, F. Cegla, P. B. Nagy, and P. Cawley, "Study and comparison of different emat configurations for sh wave inspection," *Ultrasonics, Ferroelectrics and Frequency Control, IEEE Transactions on*, vol. 58, no. 12, pp. 2571–2581, 2011.

[54] H. Gao, S. Ali, and B. Lopez, "Efficient detection of delamination in multilayered structures using ultrasonic guided wave emats," *NDT & E International*, vol. 43, no. 4, pp. 316–322, 2010.

[55] F. Li, D. Xiang, Y. Qin, R. B. Pond, and K. Slusarski, "Measurements of degree of sensitization (dos) in aluminum alloys using emat ultrasound," *Ultrasonics*, vol. 51, no. 5, pp. 561–570, 2011.

[56] K. Mirkhani, C. Chaggares, C. Masterson, M. Jastrzebski, T. Dusatko, A. Sinclair, R. J. Shapoorabadi, A. Konrad, and M. Papini, "Optimal design of emat transmitters," *NDT & E International*, vol. 37, no. 3, pp. 181–193, 2004.

[57] A. Derode, A. Tourin, and M. Fink, "Ultrasonic pulse compression with one-bit time reversal through multiple scattering," *Journal of applied physics*, vol. 85, no. 9, pp. 6343–6352, 1999.

[58] H. C. Papadopoulos, G. W. Wornell, and A. V. Oppenheim, "Sequential signal encoding from noisy measurements using quantizers with dynamic bias control," *Information Theory, IEEE Transactions on*, vol. 47, no. 3, pp. 978–1002, 2001.

[59] A. Ribeiro and G. B. Giannakis, "Bandwidth-constrained distributed estimation for wireless sensor networks-part i: Gaussian case," *Signal Processing, IEEE Transactions on*, vol. 54, no. 3, pp. 1131–1143, 2006.

Julio Isla received the Engineering degree in Telecommunications and Electronics (*summa cum laude*) and the M.Sc. degree in radio-electronics from the Instituto Superior Polytechnic José Antonio Echeverría. (ISPJAE), Cuba, in 2009 and 2012 respectively. He is currently pursuing the Ph.D. degree with the Non-Destructive Evaluation Group, Imperial College London, London, U.K.

He was with the Bioengineering Department, ISPJAE, from 2009 to 2011; the Institute of Cybernetics, Mathematics and Physics, Havana, from 2011 to 2013; and with Permasense Ltd., Horsham, U.K., from 2014 to 2016, a company that commercializes the low-power electromagnetic acoustic transducer technology that he developed with colleagues. He has also consulted for other international companies. His current research interests include low-power transduction, arrays, instrumentation, and signal processing.

This article has been accepted for publication in a future issue of this journal, but has not been fully edited. Content may change prior to final publication. Citation information: DOI 10.1109/TUFFC.2017.2661383, IEEE Transactions on Ultrasonics, Ferroelectrics, and Frequency Control

Frederic Celga was born in Freiburg im Breisgau, Germany, in 1980. He received the MEng and PhD degree in Mechanical Engineering from Imperial College London, United Kingdom, in 2002 and 2006 respectively. He returned to Imperial College London after a short stay as postdoctoral research fellow at the University of Queensland in Brisbane, Australia. In 2008 he started work at Imperial College London as lecturer in the Dynamics section of the Mechanical Engineering Department and in 2014 he was promoted to Senior Lecturer. His current research focuses on the topics of ultrasonic measurement technology, structural health monitoring and ultrasonic manipulation of particles and bubbles. He was one of the founders of Permasense Ltd. a spin out company that exploits the wall thickness monitoring technology that has been developed by him and his colleagues.